Diminishing Returns With Increasing Complexity in Reconfigurable Aperture Antennas

Rashid Mehmood, *Student Member, IEEE*, and Jon W. Wallace, *Member, IEEE*

***Abstract*—Reconfigurable aperture (RECAP) antennas hold the promise of allowing nearly arbitrary antennas to be synthesized dynamically. An important outstanding question regards the level of RECAP complexity required to capture most of the performance gains in terms of the number of reconfigurable elements (REs) per wavelength and the number of reconfiguration bits (RBs) per reconfigurable element. Diminishing improvement of beamforming performance with increasing RECAP complexity is investigated by considering a square parasitic dipole array with 9×9 elements with dimensions $1\lambda \times 1\lambda \times 0.5\lambda$. For a fixed RECAP complexity of $N_{\mathrm{RE}} N_{\mathrm{RB}}$, it is observed that having higher N_{RE} is more beneficial than high N_{RB} for dynamic beam steering, and that approximately eight REs per wavelength are required to reach diminishing performance returns.**

***Index Terms*—Antenna arrays, beam steering, complexity theory, genetic algorithms, reconfigurable antennas.**

I. Introduction

THE reconfigurable aperture (RECAP) [1], [2] is an intriguing concept, where a regular array of reconfigurable elements (REs) is manipulated to support beam steering, interference suppression, dynamic matching, filtering, frequency agility, fault tolerance, etc., with a single physical aperture. The terms *self-structuring* [3], [4] and *evolving* antennas [5] have also been used to describe a similar concept. Although RECAPs are still somewhat theoretical in nature due to losses present in current technologies for REs, future advances in microelectromechanical systems (MEMS) would allow RECAPs to revolutionize antenna and microwave engineering the way programmable logic has impacted the design of digital systems. For example, whereas antenna design for current mobile devices requires performance tradeoffs due to the large number of bands and services that must be supported in a compact form factor, RECAPs would allow the antenna to be dynamically synthesized and tailored to each application.

The purpose of this work is to explore the level of complexity required in RECAP structures to achieve near-optimal performance. The optimal efficiency and gain of antennas confined to a volume [6], [7] set an upper bound on the performance of RECAP antennas with arbitrary complexity confined to the same volume. Although it is completely expected that diminishing returns with increasing RECAP complexity will be experienced as the performance limit is approached, it is not clear at what level of complexity most of the performance gains are obtained. Also, for a limited level of complexity (which might be dictated by an application), it is interesting to study how much performance is lost compared to the optimal solution. Finally, it is of interest to understand whether complexity in the *number* or *type* of elements is more important for maximizing complexity-limited performance. These issues are addressed in this work, as well as the effects of some practical issues like bandwidth, component tolerance, and loss.

The first step toward understanding the *fundamental* dependence of performance and complexity in RECAPs should employ a simple structure that can be simulated efficiently and whose performance is not constrained by practical limitations of existing switch technology, biasing, substrate losses, etc. To this end, we consider a 9×9 half-wave dipole array used for dynamic beam steering, where a genetic algorithm (GA) is employed to focus maximum power in a specified azimuthal sector. The performance is studied with respect to increasing complexity in the number of reconfigurable elements (N_{RE}) and the number of reconfiguration "bits" per element (N_{RB}), revealing diminishing returns with increasing RECAP complexity.

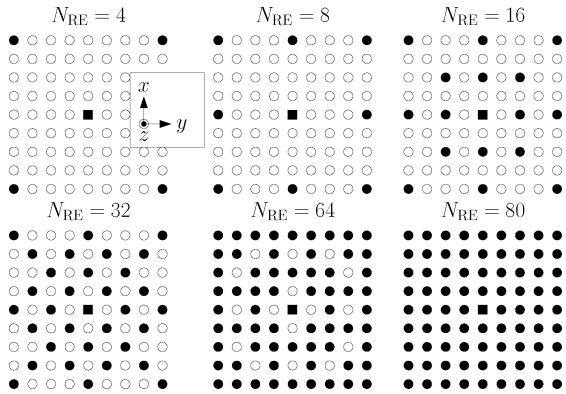

Fig. 1. RECAP structure consisting of a 9×9 dipole array, where N_{RE} elements are terminated with REs (filled circles) and the center element is the feed. Dipoles are aligned along the z-axis (extend out of the page).

II. RECAP Antenna, Simulation, and Optimization

The hypothetical RECAP structure used in this work is depicted in Fig. 1, consisting of a 9×9 square array of half-wave dipoles occupying area $1\lambda \times 1\lambda$ in the xy plane and height $\lambda/2$ in z, where the center dipole is the feeding element and other elements are terminated with reactive reconfigurable loads. The goal of the work is to study the performance of the array as both the number of loaded ports (REs) and possible states per element (reconfiguration bits, RBs) are increased.

Manuscript received February 22, 2010; accepted March 20, 2010. Date of publication April 01, 2010; date of current version April 27, 2010.

The authors are with the School of Engineering and Science, Jacobs University Bremen, 28759 Bremen, Germany (e-mail: r.mehmood@ieee.org; wall@ieee.org).

Color versions of one or more of the figures in this letter are available online at http://ieeexplore.ieee.org.

Digital Object Identifier 10.1109/LAWP.2010.2047090

A. Definition of RECAP Complexity

The complexity of the RECAP structure depends first on the number of reconfigurable elements since this defines how many digital (for switched loads) or analog (for variable reactances) outputs must be controlled. Second, complexity is also a function of the number of reconfigurable states N_{RS} that each of the REs can assume, where the number of reconfigurable bits $N_{\mathrm{RB}} = \log_2 N_{\mathrm{RS}}$ is used to conveniently define the complexity of the RE states. The total number of states for the complete RECAP is $N_{\mathrm{TRS}} = {N_{\mathrm{RS}}}^{N_{\mathrm{RE}}} = 2^{N_{\mathrm{RB}} N_{\mathrm{RE}}}$, and the total RECAP complexity is defined as $N_{\mathrm{RB}} N_{\mathrm{RE}}$, representing the number of bits required to configure all REs.

The number of REs is varied by always having all 81 antennas present, but only terminating N_{RE} of the antennas with a reconfigurable element. Having the full array of dipoles present (even when only a subset is terminated) was chosen to reduce the number of full-wave simulations and to avoid small performance differences due to a changing array structure that might overshadow the effects of RE complexity. The set of terminated antennas was chosen to try to maximize the distance between REs, thus sampling the aperture as efficiently as possible. Configurations for values of N_{RE} ranging from 4 to 80 were considered as depicted in Fig. 1.

In the following analysis, the complexity in the number of allowed states per RE was varied by considering $N_{\mathrm{RS}} \in \{2, 4, 8, 16, 32\}$. We assumed REs consisting of variable capacitances, such that the reflection coefficient presented at the kth port is $\Gamma_k = \exp(j\alpha_k)$, where $\alpha_k \in [-180^\circ, 0]$. Since the peak performance may depend on the specific set of N_{RS} states that are allowed, some consideration is required. We have found that the optimal assignment appears to be nearly uniform, or $\alpha_k \in \{0^\circ, -\Delta\alpha, -2\Delta\alpha, \ldots, -180^\circ\}$, except for $N_{\mathrm{RS}} = 2$. In the results that follow, uniform assignment of the states is used except for $N_{\mathrm{RS}} = 2$, where the best known assignment is used. Note that uniform sampling of reactance values was also tried, but this gave inferior performance.

B. Efficient Simulation of the RECAP

Optimizing the RECAP is a nonconvex problem, and a genetic algorithm is employed, requiring the network characteristics and radiation pattern of the RECAP to be computed for many thousands of candidate solutions. Since performing full-wave simulations for each configuration is computationally too expensive, we adopt a hybrid simulation procedure, where the 9×9 array is analyzed with a single method-of-moments (MoM) simulation for each port to obtain the network characteristics and embedded radiation patterns of the antennas, followed by network analysis to obtain input impedance at the feed and the resulting pattern for each specific set of parasitic loads.

MoM simulations are performed using the Numerical Electromagnetics Code (NEC), where the half-wave dipoles of radius 0.015λ are equally spaced within a $1\lambda \times 1\lambda$ area and consist of 21 segments per dipole. NEC is run for a unit voltage source across the kth port and short circuits on the other ports, yielding current $y_{jk} = i_j$, where i_j is the current flowing into the jth port. Repeating this procedure successively for each port ($k = 1, \ldots, N = 81$), the resulting matrix $\mathbf{Y}$ is the admittance matrix of the complete array. Also, when the kth port is excited, the complex vectorial far-field radiation pattern $\mathbf{E}_k(\theta, \phi)$ is stored.

Network analysis is then used to compute the input impedance and synthesized radiation pattern of the array for arbitrary loading as follows. Arranging the admittance matrix such that the feed is Port 1, and Ports 2 through N are ports for REs, we have $\mathbf{i} = \mathbf{Y}\mathbf{v}$, or

$$\begin{bmatrix} i_1 \\ \mathbf{i}_2 \end{bmatrix} = \begin{bmatrix} y_{11} & \mathbf{y}_{12} \\ \mathbf{y}_{21} & \mathbf{Y}_{22} \end{bmatrix} \begin{bmatrix} v_1 \\ \mathbf{v}_2 \end{bmatrix} \tag{1}$$

where i_1 and v_1 are the scalar current and voltage on the feed, $\mathbf{i}_2$ and $\mathbf{v}_2$ are vectors of currents and voltages on the reconfigurable ports, and $\mathbf{Y}$ has been partitioned appropriately. Terminating port $k+1$ with admittance $y_{L,k}$, $k = 1, \ldots, N-1$, we have $\mathbf{i}_2 = -\mathbf{Y}_L \mathbf{v}_2$, where $\mathbf{Y}_L$ is a diagonal matrix with $Y_{L,kk} = y_{L,k}$. Combined with (1), we have

$$\mathbf{v}_2 = -(\mathbf{Y}_{22} + \mathbf{Y}_L)^{-1} \mathbf{y}_{21} v_1 \tag{2}$$

and

$$i_1 = \underbrace{y_{11} - \mathbf{y}_{12}(\mathbf{Y}_L + \mathbf{Y}_{22})^{-1}\mathbf{y}_{21}}_{y_{\mathrm{in}}} v_1 \tag{3}$$

where y_{in} is the input admittance looking into the feed for the given termination at the REs. The realized radiation pattern of the array for feed voltage v_1 is easily found using superposition as

$$\mathbf{E}(\theta, \phi) = \sum_{j=1}^{N} v_j \mathbf{E}_j(\theta, \phi) \tag{4}$$

where voltages at the REs are found with (2). The reflection coefficient looking into the feed will also be considered, given by $\Gamma = (1 - y_{\mathrm{in}} Z_0)/(1 + y_{\mathrm{in}} Z_0)$, where the normalizing impedance $Z_0 = 72\ \Omega$ was chosen to be that of an isolated dipole.

Note that the above network-analysis technique was extensively tested by considering several configurations directly with full-wave simulations and comparing to results from network analysis, and virtually exact agreement was observed in all cases.

C. RECAP Optimization

The performance goal considered in this work is that of maximizing the fraction of available input power radiated into the vertical (θ-directed) polarization in a specified sector in the azimuthal (xy) plane, or

$$P_{\mathrm{beam}} = \frac{1}{2\pi} \int_{\phi_0 - \Delta\phi/2}^{\phi_0 + \Delta\phi/2} G(\phi) d\phi \tag{5}$$

where ϕ_0 and $\Delta\phi$ are the beam direction and width, respectively, azimuthal gain is

$$G(\phi) = (1 - |\Gamma|^2) \frac{2\pi \left| E_\theta\left(\phi, \theta = \frac{\pi}{2}\right) \right|^2}{\int_{\phi'=0}^{2\pi} \left| E_\theta\left(\phi', \theta = \frac{\pi}{2}\right) \right|^2 d\phi'} \tag{6}$$

and unless otherwise specified, $\Delta\phi = 40^\circ$.

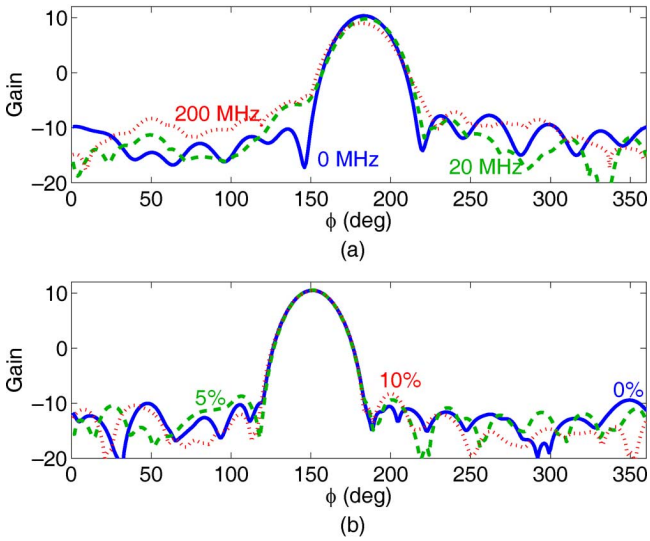

Fig. 2. RECAP gain for (a) $N_{\mathrm{RE}} = 64$, $N_{\mathrm{RS}} = 16$, $\phi_0 = 180°$ and different target bandwidths, and (b) $N_{\mathrm{RE}} = 80$, $N_{\mathrm{RS}} = 32$, $\phi_0 = 150°$, and increasing RE tolerance. Results were averaged over four runs of the GA.

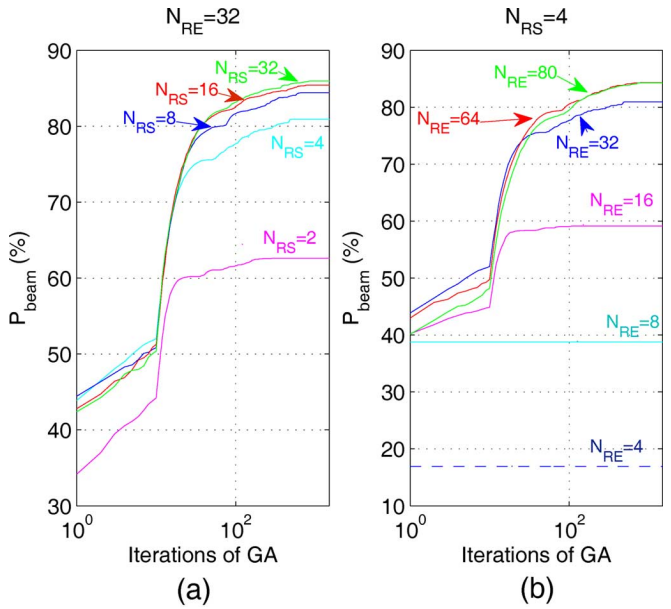

Fig. 3. Convergence in P_{beam} for (a) a fixed number of reconfigurable elements ($N_{\mathrm{RE}} = 32$), where multiple curves show increasing N_{RS} (states per RE) and (b) a fixed number of reconfigurable states ($N_{\mathrm{RS}} = 4$), with multiple curves showing increasing N_{RE}.

Since the nonconvex nature of optimizing (5) requires a global search procedure, a simple genetic algorithm was employed. Because the purpose of this work was not to optimize the genetic algorithm, but rather to use it as a tool to study performance benefit with increasing complexity, only a few details on the algorithm are given, as it is likely that other search methods would lead to very similar conclusions.

The GA herein operates by maintaining a total population of $N_I = 500$ individuals, while the number of individuals kept from one iteration to the next is $N_K = 100$. The algorithm is initialized by generating $10N_I$ random configurations for the REs, and the N_K solutions with the best fitness (highest P_{beam} for a specified sector) are kept. The algorithm progresses by combining individuals from the best N_K solutions via random crossover to generate $N_I - N_K$ children, whose RE values are then randomly changed (mutated) with a small probability. If a point of very slow improvement is detected in the algorithm, the best solution is stored, and the algorithm is restarted with a new random population. When the GA is stopped after some specified maximum number of iterations, the solution is declared to be the best solution that was found for all restarts of the algorithm. Note that for small values of $N_{\mathrm{RE}}N_{\mathrm{RB}}$, all of the RE combinations can be checked with an exhaustive search, and it was found that the GA and exhaustive search gave solutions with very similar performances.

Fig. 2 shows beamforming solutions of the GA for two different specified steering angles, not only demonstrating the beam-steering capability of the RECAP, but also the effect of finite bandwidth and tolerance. In Fig. 2(a), bandwidth W is analyzed by computing patterns at frequencies $f = f_0 = 3$ GHz and $f = f_0 \pm W/2$, and having the GA optimize average P_{beam} for these three frequencies. Capacitance (but not reactance) is assumed to be constant with frequency. The plot indicates that the GA can find solutions with useful instantaneous bandwidth. Tolerance of the REs is considered in Fig. 2(b) by perturbing the set of capacitance values with a uniform distribution, leading to a slightly different set of RSs for each RE. No obvious change in the average performance is observed, indicating that having identical RSs for the REs is not critical for adaptive RECAP beamforming.

III. Performance versus RECAP Complexity

In order to study the effect of increasing complexity on the performance of the RECAP structure, simulations were performed for all combinations of the number of reconfigurable elements $N_{\mathrm{RE}} \in \{4, 8, 16, 32, 64, 80\}$ and the number of reconfigurable states $N_{\mathrm{RS}} \in \{2, 4, 8, 16, 32\}$.

Fig. 3(a) shows the convergence of the GA for $N_{\mathrm{RE}} = 32$ and increasing number of states per RE (N_{RS}). The relatively smooth curves were obtained by averaging the results for beams synthesized at the representative angles $\phi_0 = 50°, 60°, 70°, 80°, 90°$ with 15 runs of the GA per angle. The fitness curve for a fixed value of N_{RS} has three apparent intervals: 1) the initialization phase where the population is generated randomly; followed by 2) an interval of rapid improvement in the fitness resulting from the GA; ending with 3) a final interval with diminishing improvement suggesting proximity to the optimal solution.

An important question regarding complexity in RECAPs is whether increasing N_{RS} renders finding good solutions more difficult (slower convergence). As indicated in Fig. 3(a), although the random search phase in 1) may have slower convergence due to increased complexity, the rapid improvement in interval 2) appears to be unaffected, and the increased complexity only increases the fitness of the final solution. A second effect that is clear is that the largest performance improvement comes when N_{RS} is increased from 2 to 4, and diminishing improvement is seen from 4 to 8, 8 to 16, and 16 to 32.

Fig. 3(b) plots convergence of the GA solutions for different values of N_{RE} for a fixed number of reconfigurable states per RE ($N_{\mathrm{RS}} = 4$). The straight lines for a low number of REs occur from using a simple exhaustive search. Observations are

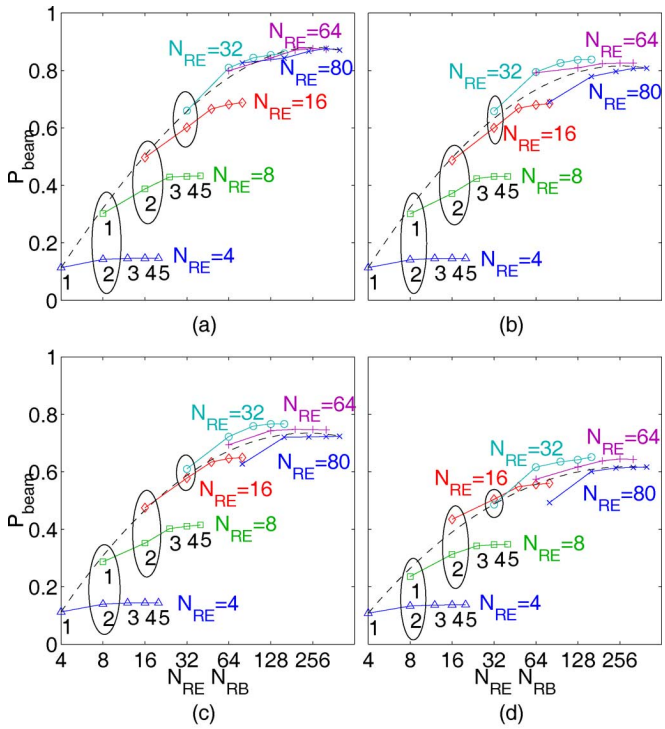

Fig. 4. Final beamforming fitness versus RECAP complexity for various series resistance values R of the REs: (a) $R = 0\Omega$; (b) $R = 0.1\Omega$; (c) $R = 1\Omega$; (d) $R = 5\Omega$. Numbers 1–5 under curves show N_{RB} values (same pattern used but not labeled in other curves). Dashed line is a fitted cubic Bezier curve showing overall trend. Circled points compare different solutions having equal complexity.

very similar to what is seen with increasing N_{RS}, or that initial convergence of the GA search is not hindered by increased complexity and that diminishing returns are seen as the number of REs in the fixed aperture are increased to a large value. Compared to Fig. 3(a), (b) also suggests that increasing the number of REs is more beneficial to performance than increasing the number of states per RE.

Fig. 4 plots the final fitness of the GA for all combinations of N_{RE} and N_{RS} versus total RECAP complexity or $\log_2 N_{\mathrm{TRS}} = N_{\mathrm{RE}} N_{\mathrm{RB}}$, where each point is an average over five angles and 15 GA runs per angle as in Fig. 3. An important concern with increasing complexity is the effect of nonideal REs that have loss, which we consider by introducing a series resistance R for each RE. In Fig. 4(a), where no loss is considered, the curves clearly show diminishing performance returns with increasing numbers of REs (N_{RE}) and number of reconfiguration bits per RE (N_{RB}). For low values of N_{RE}, the aperture is sparsely sampled, and having more REs is more beneficial than having more states for a given level of complexity.

As complexity is increased, a point is reached where only the total complexity is important, and performance increases nearly by the same amount regardless of whether N_{RE} or N_{RS} is increased. This indicates that once the aperture is sufficiently sampled with REs, doubling the number of REs is equivalent to doubling the number of reconfiguration bits per RE. Finally, it is interesting that a knee (saturation) is reached for $N_{\mathrm{RE}} = 64$, corresponding to eight REs per wavelength in each dimension, which is similar to the minimum sampling required to sufficiently capture the degrees of freedom of fields in numerical electromagnetic solvers.

Fig. 4(b)–(d) illustrate increasing loss in the REs. Although for low N_{RE} the effect is small, with increasing N_{RE} the performance saturates and then actually decreases, indicating that arbitrary complexity may not be desirable in practice. Interestingly, although total loss is higher for large N_{RE}, having a larger value of N_{RS} apparently allows some compensation of this loss. Overall, loss lowers the empirical performance versus complexity bound observed.

The effect of finite bandwidth on the performance versus complexity bound was also considered, identical to the method in Fig. 2. It was found that the main effect of a wider target bandwidth is simply a small reduction of the gain, where for bandwidths $W = 20$ and 200 MHz, a worst-case reduction of 0.4 and 1.7 dB, respectively, is seen. The relative positions of the performance-complexity curves, however, remain almost identical.

IV. Conclusion

This letter has studied the effect of limited complexity in reconfigurable aperture antennas by considering a simple square 9×9 parasitic array occupying $1\lambda \times 1\lambda \times 0.5\lambda$. Complexity of the structure is defined in terms of the number of reconfigurable elements (N_{RE}) and reconfiguration bits per element (N_{RB}). Optimizing the structure with a genetic algorithm revealed diminishing returns with increasing N_{RE} and N_{RB}, and that increasing the number of elements yields higher performance than increasing the number of states while keeping total complexity fixed. Furthermore, it was found that performance saturates for approximately eight REs per wavelength. In future work, we will apply a similar analysis of complexity for more practical planar RECAP structures with loss and biasing effects. Studying the complexity-limited performance for other criteria, such as null-steering, coupling reduction, multiple-input–multiple-output (MIMO) capacity maximization, etc., is also of high interest.

References

[1] J. H. Schaffner, R. Y. Loo, D. F. Sievenpiper, F. A. Dolezal, G. L. Tangonan, J. S. Colburn, J. J. Lynch, J. J. Lee, S. W. Livingston, R. J. Broas, and M. Wu, "Reconfigurable aperture antennas using RF MEMS switches for multi-octave tunability and beam steering," in *Proc. IEEE Antennas Propag. Soc. Int. Symp.*, Salt Lake City, UT, Jul. 16–21, 2000, vol. 1, pp. 321–324.

[2] L. N. Pringle, P. H. Harms, S. P. Blalock, G. N. Kiesel, E. J. Kuster, P. G. Friederich, R. J. Prado, J. M. Morris, and G. S. Smith, "A reconfigurable aperture antenna based on switched links between electrically small metallic patches," *IEEE Trans. Antennas Propag.*, vol. 52, no. 6, pp. 1434–1445, Jun. 2004.

[3] C. M. Coleman, E. J. Rothwell, J. E. Ross, and L. L. Nagy, "Self-structuring antennas," *IEEE Antennas Propag. Mag.*, vol. 44, no. 3, pp. 11–23, Jun. 2002.

[4] C. M. Coleman, E. J. Rothwell, and J. E. Ross, "Investigation of simulated annealing, ant-colony optimization, and genetic algorithms for self-structuring antennas," *IEEE Trans. Antennas Propag.*, vol. 52, no. 4, pp. 1007–1014, Apr. 2004.

[5] D. S. Linden, "Evolving antennas in-situ," *Soft Comput., Fusion Found., Method. Appl.*, vol. 5, pp. 1432–7643, Apr. 2004.

[6] R. C. Hansen, "Fundamental limitations in antennas," *Proc. IEEE*, vol. 69, no. 2, pp. 170–182, Feb. 1981.

[7] M. Gustafsson, C. Sohl, and G. Kristensson, "Illustrations of new physical bounds on linearly polarized antennas," *IEEE Trans. Antennas Propag.*, vol. 57, no. 5, pp. 1319–1327, May 2009.